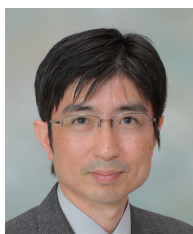


Highlight Review**Recent Progress in Quinoidal Singlet Biradical Molecules**

Takashi Kubo

Department of Chemistry, Graduate School of Science, Osaka University,
1-1 Machikaneyama, Toyonaka, Osaka 560-0043

(E-mail: kubo@chem.sci.osaka-u.ac.jp)



Takashi Kubo was born in Yamaguchi, Japan, in 1968. He graduated from Osaka University in 1991, received M.Sc. in 1993 under the guidance of Professor Ichiro Murata, and received Ph.D. in 1996 under the guidance of Professor Kazuhiro Nakasuji. After working at Mitsubishi Chemical Co., he joined Professor Nakasuji's group at Department of Chemistry, Graduate School of Science, Osaka University in 2000 as Assistant Professor. In 2006 he served as Associate Professor. Since 2006 he is Professor of Graduate School of Science, Osaka University. He received the Bulletin of the Chemical Society of Japan Award in 2001. His research interests are structural and physical organic chemistry, mainly the syntheses and properties of polycyclic aromatic compounds with open-shell character, and the development of multifunctional materials using a cooperative proton- and electron-transfer system.

Abstract

Elusive nature in spin state is a feature of singlet biradical molecules and arises from the weak coupling of unpaired electrons. This highlight review focuses on recent advances in experimental approaches for elucidating the electronic structure and properties of singlet biradical molecules having quinoid skeletons.

Introduction

As pointed out by Szwarc,¹ the definition of biradical is more difficult than that of monoradical. According to his criterion, a biradical is a neutral molecule endowed with two unpaired electrons (and therefore paramagnetic). Actually, biradicals can be divided into two categories in terms of spin multiplicity, i.e. triplet biradical and singlet biradical, and the former fulfills the criterion. However, singlet biradical seems to be not so definitive, because “unpaired” electrons can be coupled covalently within a molecule. Some singlet biradicals show paramagnetic (open-shell) behaviors in chemical reactivity and magnetic measurements, and some similar to normal closed-shell compounds, which depends on the π -conjugation scaffold connecting two spin centers.

The molecule that has played an important role in singlet biradical chemistry is *p*-quinodimethane (**1**) (Figure 1). The generation of **1** was first achieved in 1947 by the pyrolysis of *p*-xylene.² **1** was stable in the gas phase, whereas labile in the condensed phase to give rise to an insoluble material, which is mainly poly(phenylenevinylene). Later it was found that the insoluble material also includes [2.2]paracyclophane.³ Exposure of the pyrolysis product to iodine in the gas phase afforded *p*-xylylene diiodide. All these biradicaloid behaviors imply the open-shell character of **1** in the ground state, which attracted the attention of theoreticians; but Coulson demonstrated, using the Hückel molecular orbital (HMO) calculation, that the ground state of **1** possesses a closed-shell quinoid form with very large free valence (that is, radical reactivity) at two terminal methylene carbons.⁴ The quinoid ground state for **1** was also confirmed by ¹H NMR,⁵ UV-vis,⁶ IR,^{6,7} Raman,^{7,8} photoelectron,⁹ and electron diffraction¹⁰ measurements. On the other hand, it is unlikely that a triplet biradical species causes the biradicaloid chemical behaviors, because a CASSCF(8,8)/6-31+G(d) calculation predicted a singlet-triplet energy gap (ΔE_{S-T}) of 159 kJ mol⁻¹.¹¹ The biradicaloid behaviors of **1** appears not to arise from the biradical electronic structure.

Similar elusive nature is also seen in π -extended quinodimethane, Chichibabin's hydrocarbon (**2**) (Figure 2). In 1907, Chichibabin isolated **2** as a blue-violet compound that reacts readily with oxygen.¹² Many measurements were carried out to characterize the electronic structure of **2**, but these studies

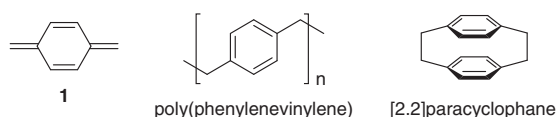


Figure 1. *p*-Quinodimethane (**1**), and its polymeric and dimeric compounds.

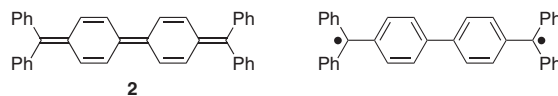


Figure 2. Chichibabin's hydrocarbon (**2**). (Left) Kekulé form and (right) biradical form.

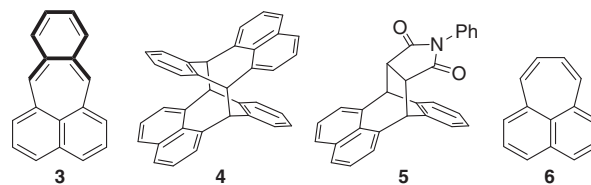


Figure 3. Pleiadene (**3**), its dimer (**4**), Diels-Alder adduct (**5**), and pleiadene (**6**).

caused controversial discussions on its spin state: singlet, triplet, or double doublets. Although magnetic susceptibility measurements indicated that **2** is diamagnetic,¹³ a solution ESR measurement suggested that ca. 4% of the molecule is in the paramagnetic triplet state at 300 K.¹⁴ Another solution ESR study by Jarrett et al. demonstrated that the interaction between the two unpaired electrons is weak because sharp hyperfine lines were observed in the spectrum.¹⁵ An ESR study by Reitz and Weissman also supported the weakness of the interaction.¹⁶ However, the weak coupling is inconsistent with the diamagnetic behavior and the small amount (ca. 4%) of triplet species, evoking the issue “The Biradical Paradox.”¹⁷ In 1964, this controversial issue was partially resolved by further ESR studies, from which it was concluded that the paramagnetic species are derived from a dimer or higher polymer of **2**,¹⁸ and in 1969 a hydrogen abstracted molecule was proposed as another candidate for the paramagnetic species on the basis of ENDOR studies by Brauer et al.¹⁹ The conclusive remark was finally given by Montgomery et al. in 1986,²⁰ who demonstrated that **2** adapts a singlet quinoidal structure with an apparent manifestation of biradical character in the ground state, by X-ray single-crystal analysis. An ESR measurement of the pure **2** gave no signal at 77 K.

Pleiadene (**3**) is also a compound that has been investigated in terms of singlet biradical character. **3** was first generated by Cava et al. in 1963, as a reactive intermediate, by the pyrolysis of a sulfone precursor²¹ and was isolated in dimeric form **4** or as Diels-Alder adduct **5** in the presence of *N*-phenylmaleimide.²² These reactivities apparently come from the *o*-quinoid structure (highlighted in bold line in Figure 3), because pleiadene (**6**) is thermally stable²³ and unaffected by maleic anhydride at 80 °C.²¹ Generation of **3** in a milder condition and photochemical synthesis in a low-temperature matrix was performed by Michl et al. in 1970.²⁴ Irradiation of a cyclobutene precursor in a 3-methylpentane glass afforded a stable yellow-green **3**, which disappeared in 10–15 s at the glass-melting temperature (110 K). The product was the dimer **4** and the mechanism of the rapid reaction from two **3** to **4** is quite interesting because it is formally a thermally forbidden [4 + 4] cycloaddition. A stepwise radical reaction might be more plausible, but Michl proposed that the concerted mechanism is also a compelling path if the transition state bears biradicaloid character. From a quantum chemical calculation, **3** possesses a low-lying doubly excited

configuration, which is closely related to singlet biradical character, and the admixing of the ground state configuration with the doubly excited configuration would make the transition state lower in energy. The state dominated by the doubly excited configuration was found to be low-lying by using UV-vis spectroscopy and a PPP-CI calculation.^{25,26}

In this way, compounds with singlet biradical character show unique behaviors in reactivity and physical properties due to the unordinary electronic structure, which have attracted the interest of synthetic, physical, and theoretical chemists, but sometimes give misleading results due to the contamination of decomposed products. Stability is an important factor for the characterization of singlet biradical compounds by various measurement methods and also for applications in many different fields. This review focuses mainly on recent advances in experimental approaches for understanding the electronic structure of stable singlet biradical compounds.²⁷

Theoretical Treatment of Singlet Biradical Character

Although biradicaloid compounds feature high reactivity, a low-energy absorption band, broadening of NMR signals, small ΔE_{S-T} , and a low-lying doubly excited state, these properties are too phenomenological to be a criterion of singlet biradical character. The amount of singlet biradical character would be an important factor for understanding the nature of singlet biradical species. The natural orbital (NO) is a key concept for estimating the amount, and its occupation number (NOON) is a good index of singlet biradical character.²⁸ The NOON values can be calculated by CASSCF or broken symmetry (BS)²⁹ UDFT calculation methods and the NOON of the lowest unoccupied natural orbital (LUNO) corresponds to the amount of singlet biradical character (y). For instance, a CASSCF(2,2)/6-31G calculation shows that *p*-quinodimethane (**1**) possesses a NOON of 0.097 for LUNO, leading to a y of 9.7%. A UHF-based approach was also developed by Yamaguchi;³⁰ the y value can be determined from the following equations: $y = 1 - 2T / (1 + T^2)$, $T = (n_H - n_L) / 2$, where n_H and n_L represent the occupation numbers of HONO and LUNO, respectively. Theoretical treatment of singlet biradical character is well summarized in the literature.^{31,32}

Properties of Stable Singlet Biradicals

Bisphenalenyls. The intrinsic stability of singlet biradical species can be attained by the delocalization of formally appearing unpaired electrons. Because quinodimethanes are an important building block to develop singlet biradical character, the combination of quinodimethanes and spin-delocalizing scaffolds would lead to the stabilization of singlet biradicals. Following this design concept, a molecule **7** was designed, which consists of *p*-quinodimethane and two phenalenyl moieties (Figure 4). In **7**, the phenalenyl ring acts as a spin-delocalizing unit, because its highly symmetric structure (D_{3h}) enables an unpaired electron to fully delocalize over the ring. The quinoid Kekulé form **7** would resonate well with the biradical form **7'** by virtue of aromatic sextet formation, and then, the unpaired electrons emerging on the terminal carbons of the *p*-quinodimethane moiety can delocalize over the phenalenyl

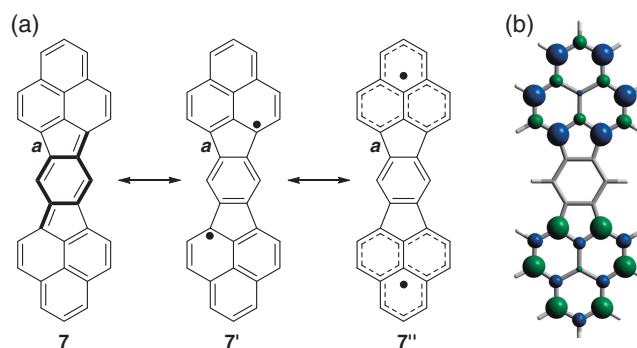


Figure 4. (a) Resonance formula of **7**. (b) Spin density map of **7**.

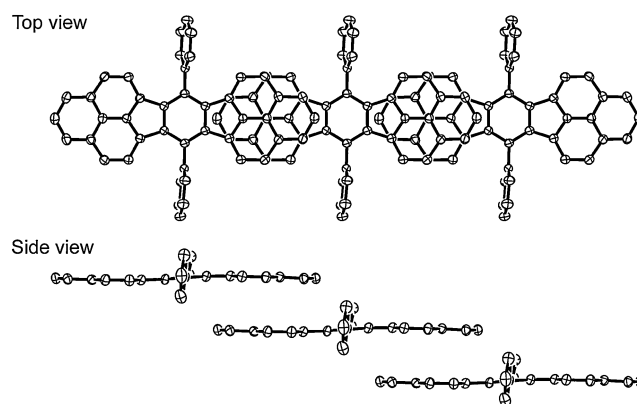


Figure 5. One-dimensional stack of **8**.

rings (**7''**). The highly delocalized spin structure of **7** was supported by a BS-UB3LYP calculation (Figure 4b) that shows a biradical index y of 37%.

Kubo et al. prepared a diphenyl derivative **8** in 16 steps from acenaphthene.³³ The stability of **8** is quite high; a solution of **8** showed no appreciable decomposition for a couple of weeks in air at room temperature. The solution ¹H NMR spectrum of **8** showed very broad signals for aromatic protons at room temperature, and upon cooling, progressive line sharpening was observed. A thermally excited triplet species is responsible for signal broadening and indeed the small ΔE_{S-T} of 18 kJ mol⁻¹ was confirmed by SQUID measurements. The electrochemically determined HOMO–LUMO gap was only 1.15 eV. All these properties are in line with the characteristics of singlet biradicals.

As mentioned above, pleiadene (**3**) undergoes a thermally forbidden [4 + 4] dimerization at low temperature in the dark. This strong propensity to form covalent bonds between molecules might be a characteristic feature of singlet biradical species. Actually, the stacking motif of **8** in the solid state was strongly affected by an intermolecular covalent bonding interaction. Recrystallization of **8** from a chlorobenzene solution afforded single crystals and X-ray crystallographic analysis revealed that **8** forms a one-dimensional (1D) stack of superimposed phenalenyl rings. The average π – π separation distance (R) between the overlapping phenalenyls is 3.137 Å (Figure 5), which is much smaller than the sum of the van der Waals radius

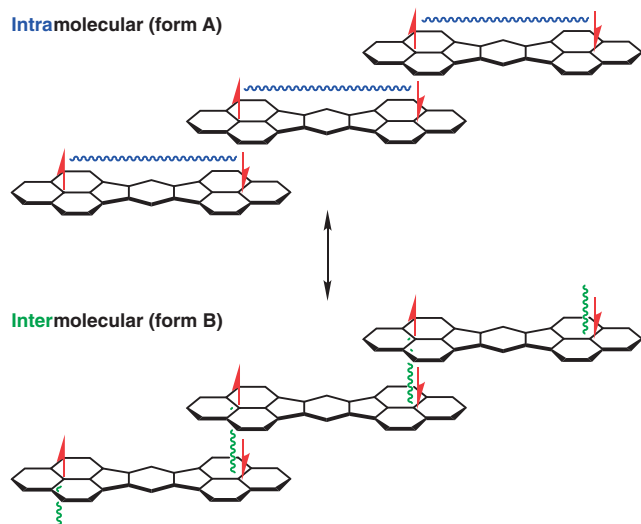


Figure 6. Resonance formula for describing the electronic structure of the 1D stack of **8**. Blue and green wavy lines represent intra- and intermolecular covalent bonding interactions, respectively.

of carbon atom (3.4 Å). The short contact is ascribable to an intermolecular covalent bonding interaction of two unpaired electrons that appear in the resonance formula shown in Figure 4.

A dilute CH_2Cl_2 solution of **8** showed an intense HOMO–LUMO absorption band at 746 nm and the formation of a 1D stack caused a large red shift of the band by 6600 cm^{-1} . In the 1D stack, a covalent bonding interaction works between the molecules as well as within the molecule and the coexistence of the interactions causes electron delocalization over the 1D stack, resulting in a large red shift. The electronic structure of the 1D stack can be described by the resonance hybrid of intramolecular (form **A** in Figure 6) and intermolecular (form **B**) covalent bonding interactions.

The contribution weight of **A** and **B** can be regulated by changing the separation distance between the overlapping phenalenyl rings. A dimethyl derivative **9** was a good model compound for the purpose (Figure 7). **9** afforded single crystals that incorporate many kinds of recrystallization solvents (benzene, toluene, and chlorobenzene).³⁴ X-ray measurement revealed that the crystal including benzene shows the smallest distance ($R = 3.160\text{ Å}$, Table 1) at 200 K. At the same temperature a larger separation ($R = 3.225\text{ Å}$) was observed for the crystal including chlorobenzene (PhCl), and the separation distance changed by changing the measurement temperature. An extreme case, that is, $R = \infty$, was obtained with the crystal including toluene, because there was no overlap between phenalenyl rings. Interestingly, there is a strong correlation between the separation distance R and the length (L) of the linker bond (a) that connects the phenalenyl ring and the central benzene ring; the bond a elongates as the overlapping phenalenyl rings come close. The length of a is related to the strength of the intramolecular covalent bonding interaction, because the π -bond order of a is 0.5 for the Kekulé form and zero for the biradical form (Figure 4). The stronger the covalent bonding interaction becomes between the molecules (form **B**)

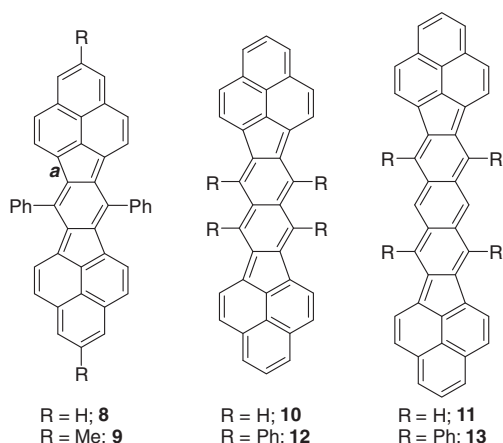


Figure 7. Derivatives of benzoquinoid **8** and **9**, naphthoquinoid **10** and **12**, and anthraquinoid **11** and **13** bisphenalenyls.

Table 1. The π – π separation distances (R) between overlapping phenalenyl rings and the lengths (L) of the bond a , in the crystals of **9**

	Solvates				
	Benzene	PhCl	PhCl	PhCl	Toluene
T/K^a	200	100	200	300	200
$R/\text{Å}$	3.160	3.208	3.225	3.279	n.d. ^b
$L/\text{Å}^c$	1.476(2)	1.472(2)	1.469(2)	1.465(3)	1.457(2)

^aX-ray measurement temperatures. ^bNo overlap was observed.

^cMean values.

and the weaker within the molecule (form **A**). Optical spectra were also affected by the separation distance R . The reflection spectra of a single crystal of **9**/PhCl showed a blue shift upon cooling. This means that a stronger intermolecular interaction leads to a wider gap between the valence and conduction bands. In principle, when alternating electron–electron interactions are well balanced, the band gap becomes vanished. For instance, the Hückel theory predicts a zero band gap for an infinite polyene with no bond length alternation. The wider gap observed in **9**/PhCl at lower temperatures suggests that the contribution weight of form **B** is larger than that of form **A** in the 1D stack of **9**.

Replacement of the central benzene ring in **7** with naphthalene and anthracene rings will lead to a more enhanced singlet biradical character (Figure 7), because naphthalene and anthracene have a larger aromatic stabilization energy than benzene. A broken-symmetry UB3LYP/6-31G** calculation showed that bisphenalenyls with naphthoquinoid **10** and anthraquinoid **11** skeletons possess 56% and 62% of singlet biradical character (γ) in the ground state, respectively. Tetraphenyl derivatives **12** and **13** of **10** and **11** were prepared by multistep syntheses.^{35,36} X-ray analysis revealed that **12** and **13** form 1D stacks in a slipped stacking arrangement with a superimposed phenalenyl overlap, which was almost identical to that of **8** and **9** (Figure 8). Very short π – π contacts (3.170 Å for **12**, 3.122 Å for **13**) were also observed.

The solids **12** and **13** showed absorption bands in the near-infrared (NIR) region, which were shifted to a lower energy region relative to the solution HOMO–LUMO absorption bands owing to the coexistence of intra- and intermolecular covalent

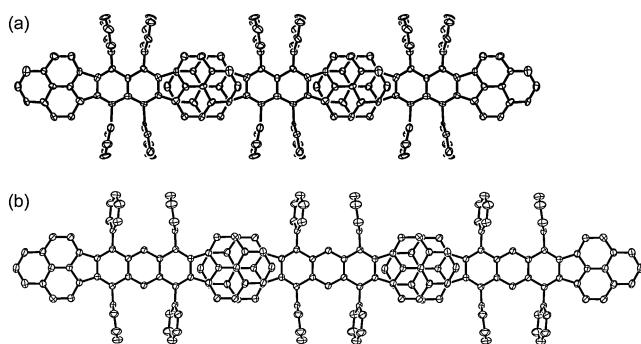


Figure 8. One-dimensional stack of (a) **10** and (b) **11**.

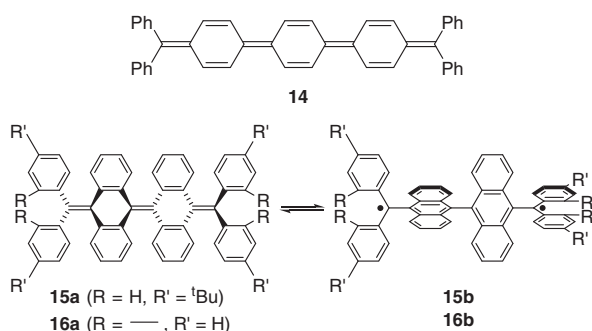


Figure 9. Müller's hydrocarbon (**14**). Tetrabenzo Chichibabin's hydrocarbons (**15** and **16**).

bonding interactions in the 1D stacks. However, the NIR bands observed in the solid state shifted to a higher energy region with increasing singlet biradical character: 1440 nm for **8**, 1280 nm for **12**, and 1025 nm for **13**. This higher energy shift can be explained in terms of that the intra- and intermolecular covalent bonding interactions become more unbalanced for larger singlet biradical systems.

Extended Quinoids and Quinones. As mentioned above, Chichibabin's hydrocarbon (**2**) possesses appreciable singlet biradical character. The insertion of quinoid units into **2** would lead to more enhanced biradical character and indeed a tris-quinoid system **14** (namely, Müller's hydrocarbon, Figure 9) was prepared and characterized by ESR.³⁷ **14** showed an ESR signal typical for triplet species at 153 K ($|D| = 0.0035 \text{ cm}^{-1}$, $|E| < 0.002 \text{ cm}^{-1}$), and from the temperature dependency of signal intensities, ΔE_{S-T} was determined to be only ca. 4 kJ mol^{-1} . Benzannulation of the central quinoid moieties also affects the magnetic properties of **2**. Recently two types of tetrabenzo derivatives **15** and **16** of **2** were isolated by Wu and their biradicaloid behaviors were thoroughly investigated by means of X-ray crystallographic and spectroscopic measurements.³⁸ The interesting point of the benzannulated compounds lies in that the electronic structure of the ground state is determined by the energy balance between structural strain and π -bond formation. Due to the steric hindrance around the anthracene moiety, **15** and **16** adapt not a planar form but an orthogonal or folded form as the most stable form. The reduction of a diol precursor of **15** afforded the orthogonal biradical form **15b**, which gradually transformed into the folded quinone form **15a** with a half-life time of 495 min. In contrast, the fluorenyl-

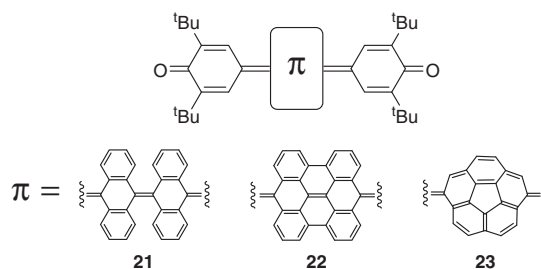
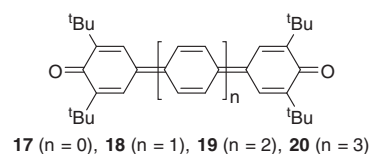
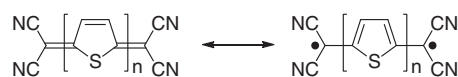


Figure 10. π -Extended quinones.

terminated **16** adapted only the orthogonal biradical form **16b** that has a very small ΔE_{S-T} of -1.4 kJ mol^{-1} . The difference in conformation between **15** and **16** is ascribable to the difference of steric strain around the terminal double bonds. The rigid fluorenyl suffers from larger strain in the folded form, leading to a larger energy difference between the folded and the orthogonal forms.

Biphenoquinone (**17**) and terphenyloquinone (**18**) are air stable and diamagnetic compounds (Figure 10). According to X-ray analysis, **18** adapted a nearly planar form with a large bond length alternation in the quinoid framework, and showed no detectable ESR signal in the solution and solid state.³⁹ In contrast, the presence of ESR signals in the solution and solid states for quaterphenyloquinone (**19**)⁴⁰ and quinquephenyloquinone (**20**)⁴¹ implies that these compounds have appreciable biradical character. Because **19** and **20** appear to adapt predominantly a diamagnetic quinoid form in the solid state by SQUID measurements, thermally excited triplet species may be responsible for the solid-state ESR signals. On the other hand, in solution, the rotation of the quinoid moieties would result in the decoupling of two unpaired electrons, giving rise to the ESR signals. The replacement of the quinoid framework with other π -conjugate systems affects the structure and property of the quinone system. Anthracene- and bisanthene-inserted quinones **21** and **22**, which were isolated by Wu,⁴² showed folded and twisted quinone forms, respectively. Due to the rigid framework of bisanthene, **22** prefers a twisted form over a folded form. **21** and **22** showed sharp NMR signals even at elevated temperature, indicating the closed-shell ground state. In contrast, a corannulene-inserted quinone **23** showed biradical properties: a triplet ESR signal in a rigid glass and small ΔE_{S-T} of 3.4 kJ mol^{-1} .⁴³

Systematic investigation in terms of singlet biradical character was intensively carried out for thienoquinoid compounds. Otsubo et al. prepared a series of dicyanomethylene-terminated thienoquinoids **24–29** (Figure 11) and revealed that **28** and **29** shows no NMR signal; instead, ESR signals are observed. From the ESR signal intensity, the fractions of magnetic species were estimated to be 2.8% for **28** and 29% for **29**.⁴⁴ The species that gave ESR signals would be thermally excited triplet species, because triplet populations estimated from the theoretical ΔE_{S-T} (10.9 kJ mol^{-1} for **28**, 5.65 kJ mol^{-1}



24 ($n = 1$), **25** ($n = 2$), **26** ($n = 3$), **27** ($n = 4$), **28** ($n = 5$), **29** ($n = 6$)

Figure 11. Resonance formula of dicyanomethylene-terminated thienoquinoids **24–29**.

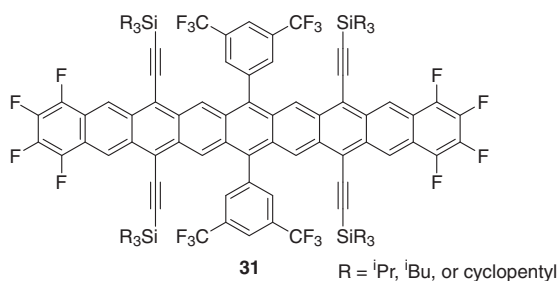
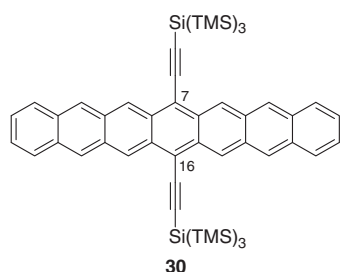
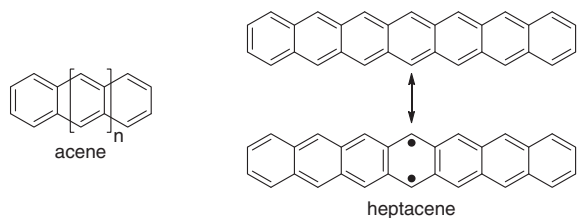


Figure 12. Acenes and resonance formula of heptacene.

for **29**) and a Boltzmann distribution are 3.6% for **28** and 24% for **29**. Singlet biradical contribution to the ground state was investigated by using Raman spectroscopy.⁴⁵ Raman spectra measured at 123 K revealed that the small systems give quinoidal Raman bands, whereas the bands of the larger systems move into the aromatic region. The contribution weight of the aromatic biradical form to the ground state increases with increasing the number of a thienoquinoid unit.

Acenes, Anthenes, and Graphene Nanoribbons.

Acenes (Figure 12), which are composed of linearly fused benzene rings, have attracted much attention due to high reactivity and deep color. These unique properties, which are often contrasted with angularly benzene-fused systems, phenacenes, can be understood by the concept of Clar's aromatic sextet (Clar sextet), which well explains the physical and chemical properties of many kinds of polycyclic compounds.⁴⁶ In acenes, only one circle, which is the notation of the Clar sextet, can be written and furthermore the migration of the circle into adjacent rings "dilutes" the stabilization effect of the aromatic sextet. Therefore, the stability and the HOMO–LUMO

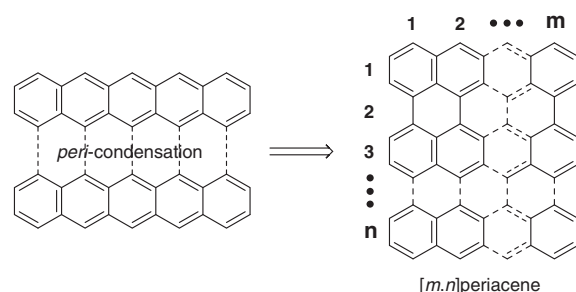


Figure 13. Structure of $[m.n]$ periacene.

energy gap of acenes drastically decrease with increasing the number of benzene rings. The contact between singlet biradical character and those unique behaviors of acenes has been first invoked by Bendikov et al. in 2004.⁴⁷ They predicted that the open-shell singlet is the lowest state in acenes larger than hexacene, and they behave as singlet biradicals, whose singly-occupied molecular orbital (SOMO) is populated on their zigzag edges, by using a broken symmetry UB3LYP/6-31G* method. The parent heptacene has not been isolated in pure form, but in 2006, Neckers et al. succeeded in the generation of parent heptacene in a poly(methyl methacrylate) (PMMA) matrix by the photo-decarbonylation of a diketone precursor.⁴⁸ Irradiation at 395 nm gave the longest wavelength absorption centered at 760 nm (1.63 eV). Full spectroscopic characterization of heptacene was achieved by the introduction of tris(trimethylsilyl)-silylacetylene groups at 7,16-positions (**30**), which makes heptacene soluble and stable.⁴⁹ The crystal structure was also determined. The electronic absorption spectrum and cyclic voltammogram gave HOMO–LUMO gaps of 1.36 eV (912 nm, estimated from the absorption edge) and 1.30 eV. ¹H and ¹³C NMR signals of the substituted heptacene are still sharp, indicating a closed-shell ground state, in contrast to the singlet open-shell character predicted by the broken symmetry UB3LYP calculation. Biradicaloid behavior was observed for substituted nonacenes **31**.⁵⁰ The optical HOMO–LUMO gap was determined to be 1.2 eV, which was almost the same as the electrochemical HOMO–LUMO gap (1.19 eV). These small HOMO–LUMO gaps suggest the singlet biradical character of nonacene. Actually, the ¹H NMR spectrum of **31** gave no signal in the aromatic region due to the existence of magnetic species, probably thermally excited triplet species.

The *peri*-condensation of acenes leads to rectangular PAHs, which are referred to as periacenes. The number of six-membered rings in each direction of the linear and angular ring-fusion is indicated in brackets as $[m.n]$ (Figure 13). The amount of singlet biradical character (γ) of $[m.n]$ periacene was calculated by using the index defined by Yamaguchi³⁰ coupled to the symmetry-broken UBHandHLYP/6-31G* calculation.⁵¹ Table 2 shows the γ values of acenes and $[m.n]$ periacene. [3.3]periacene, namely bisanthene, has small γ (12%), suggesting that the molecule can be classified into a closed-shell molecule. A larger homolog, [3.5]periacene (namely teranthene), gives a large value of γ (59%), clearly indicating appreciable singlet biradical character. Larger systems, in the right lower region of Table 2, possess perfect singlet biradical character. Periacenes isolated in crystalline form so far are very limited: only [3.3]-, [3.5]-, and [3.7]periacene. [5.3]periacene, namely

Table 2. Singlet biradical character γ of acenes and $[m.n]$ periacenes

n	m					
	2	3	4	5	6	7
1	0.00	0.00	0.01	0.07	0.20	0.40
3	0.00	0.12	0.60	0.84	0.94	0.98
5	0.01	0.59	0.91	0.98	0.99	1.00
7	0.05	0.84	0.98	1.00	1.00	1.00

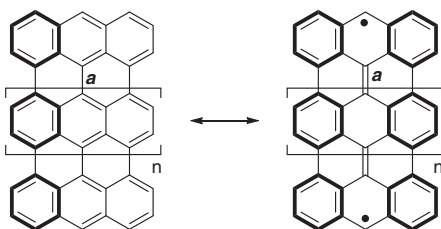


Figure 14. Resonance formula of anthenes. The six-membered rings depicted by bold lines represent the Clar sextets.

peripentacene, was detected in the gas phase by mass spectroscopy,⁵² and the isolation of a derivative was also attempted by Müllen et al.⁵³

For understanding the singlet biradical character of $[3.n]$ periacenes, namely anthenes, the resonance formula consisted of Kekulé and biradical forms is helpful (Figure 14). In the formula, two unpaired electrons appear on both *meso*-positions of anthenes, when one draws the structure with a maximum number of Clar sextets, and at the same time, the bonds denoted by *a* assume double bond character. Therefore, the singlet biradical contribution to the ground state would lead to the shortening of the bonds *a*.

A tetra-*tert*-butyl derivative of bisanthene, **32** (Figure 15a), was isolated and characterized by X-ray crystallographic, electrochemical, and spectroscopic methods. X-ray crystallographic analysis of **32** showed a length of 1.451(2) Å for the bond *a*,⁵⁴ which is identical to the regular C(sp²)-C(sp²) single bond length (1.45 Å). This means that bisanthene has very small singlet biradical character in the ground state. The relatively large HOMO-LUMO gap (1.87 and 1.68 eV determined by optical and electrochemical methods) and large ΔE_{S-T} (52.4 kJ mol⁻¹ calculated by a UB3LYP method) are consistent with the small biradical character. This closed-shell nature of **32** is also supported by a variable temperature ¹H NMR experiment, which showed no signal broadening of the aromatic protons even at 383 K (Figure 15b).

Anthene that three anthracenes are *peri*-condensed is called teranthene. A kinetically stabilized teranthene (**33**) (Figure 16a) was isolated and characterized in 2010.⁵⁵ X-ray crystallographic analysis of **33** showed a relatively short length (1.424(4) Å) in the bond *a*, indicating a large double bond character for this bond. In addition, the side six-membered rings had a large benzenoid character, because the harmonic oscillator model of aromaticity (HOMA) values,^{56,57} which is the geometry-based aromaticity index, were close to unity (0.854 and 0.832), as shown in Figures 16b and 16c. These experimental findings suggest a large contribution of the biradical form to the ground

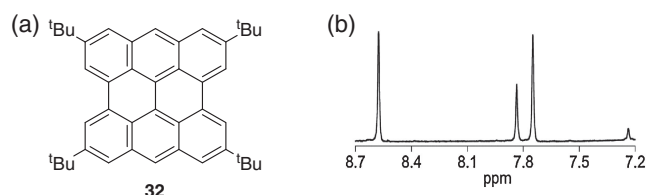


Figure 15. (a) Tetra-*tert*-butylbisanthene (**32**). (b) ¹H NMR spectrum of **32** at 383 K.

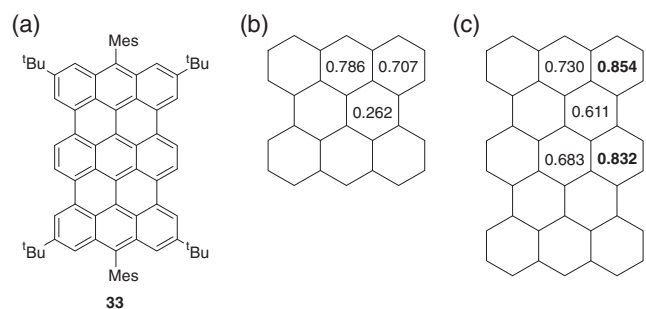


Figure 16. (a) Tetra-*tert*-butyl dimesityl teranthene (**33**). HOMA values of (b) **32** and (c) **33** determined from X-ray structures.

state. The ¹H NMR spectrum of **33** showed severe line broadening at room temperature, and upon cooling, progressive line sharpening was observed. Thermally excited triplet species would be responsible for the signal broadening and the small ΔE_{S-T} was determined to be 16.0 kJ mol⁻¹ by SQUID measurements. The electronic absorption spectrum of **33** showed an intense absorption band at 878 nm (ϵ 97800), accompanied by a broad and weak band centered at 1054 nm (ϵ 8000). The former intense band can be assigned to a HOMO \rightarrow LUMO single excitation, while the latter a HOMO,HOMO \rightarrow LUMO,LUMO double excitation, according to a strongly contracted second-order *n*-electron valence state perturbation theory (NEVPT2) calculation that allows multielectron excitation.⁵⁸ Actually, one signature of biradicaloid character is the presence of a low-lying excited singlet state dominated by the doubly excited configuration. Negri et al. reported that a weak low-energy band was observed for thienoquinoid compounds with large biradical character.⁵⁹

The reason why bisanthene has negligible biradical character while that of teranthene is appreciable is as follows. Upon transforming from the Kekulé to the biradical form for anthenes, one C-C π -bond is cleaved, as shown in Figure 14. The destabilization energy due to π -bond cleavage is ca. 270 kJ mol⁻¹.⁶⁰ At the same time, some aromatic sextets are newly generated during the transformation. The aromatic stabilization energy of benzene, based on the homodesmotic stabilization energy, is ca. 90 kJ mol⁻¹.^{61,62} For bisanthene, the destabilization energy of π -bond cleavage is not compensated by the formation of additional sextets since the additional sextets in the biradical form are only two; thus the Kekulé form has dominant contribution to the ground state in bisanthene. On the other hand, for teranthene, the difference of the sextets upon transformation comes to three. The destabilization and stabilization energies are well balanced, resulting in a large contribution of the biradical form to the ground state.

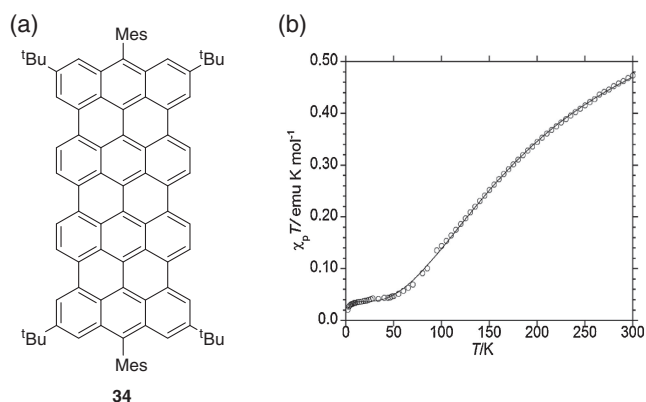


Figure 17. (a) Tetra-*tert*-butyldimesitylteranthene (**34**). (b) χT - T plot for the powdered **34**.

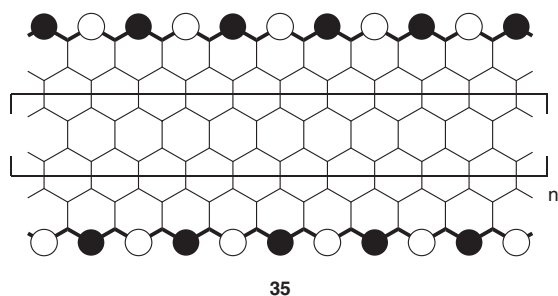


Figure 18. Edge-localized nonbonding π -state of ZGNRs (**35**).

A quadruply *peri*-condensed system is called quateranthene, which has γ of 84% at the UBHandHLYP level of calculation. A kinetically stabilized derivative **34** (Figure 17a) was prepared and isolated in crystalline form.⁶³ X-ray crystallographic analysis revealed that the bond *a* of **34** is quite short (1.416(3) Å in average), supporting the very large singlet biradical character. The ¹H NMR spectra of **34** gave no signals from the main core ring even at 183 K. The ΔE_{S-T} determined by SQUID measurements (Figure 17b) was only 2.9 kJ mol⁻¹, from which the population of the triplet species of **34** is estimated to be ca. 50% at room temperature. Due to the high population of the triplet species, the UV-vis-NIR spectrum of **34** showed temperature-dependent behavior. However, the spectral changes were small; a low-energy band at 920 nm observed at 300 K bathochromically shifted only by 50 nm at 180 K along with an isosbestic point. The similarity of the spectra may indicate a similar distribution of unpaired electrons around the *meso*-positions in the singlet and triplet states.

These biradical properties of anthenes are closely related to the “edge state” in zigzag-edged graphene nanoribbons (ZGNRs, **35**), which is a peculiar magnetic state originating from an electron–electron correlation in an edge-localized nonbonding π -state (Figure 18). The edge state has been attempted to be observed by various experimental measurements,^{64–72} and especially, scanning tunneling microscopy and spectroscopy (STM/S) have achieved to propose good evidence of the edge state around the zigzag edges in GNRs.^{64,65,72} The edge localization was first understood by a physics approach, that

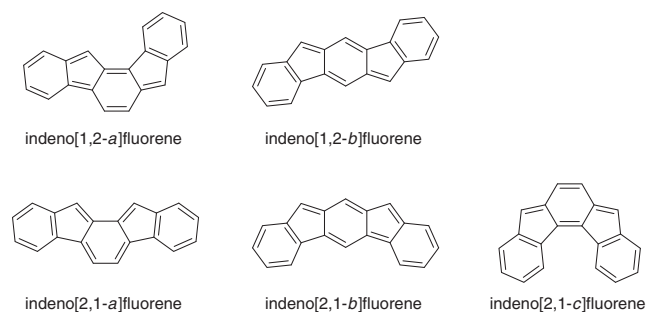


Figure 19. Indenofluorene family.

is, by a tight binding band calculation combined with a Hubbard model.^{73–75} On the other hand, unveiling the mechanism of edge localization of unpaired electrons in anthenes is a bottom-up chemical approach. Aromatic sextet formation is a key mechanism of the magnetic state of anthenes, and this classical and simple idea would indeed dominate the electronic structure of nanographenes.

Indenofluorenes. Indenofluorenes, which are 6-5-6-5-6 ring systems, possess characteristic features of peripheral 20π electrons along with quinoid structures. Indenofluorenes have five possible regioisomers as shown in Figure 19, and all these compounds, except for indeno[1,2-*a*]fluorene, have been isolated in crystalline form by the introduction of bulky substituents.

The most extensively studied isomer is indeno[1,2-*b*]fluorene. Although full characterization of the unsubstituted indeno[1,2-*b*]fluorene has not been reported yet, in 2011, Haley et al. succeeded in X-ray structural characterization of TIPS-acetylene derivatives **36**.⁷⁶ These blue-violet compounds are stable in an air-saturated solution state under light and their lifetimes are 2–3 months. The primary interest of the indenofluorene family is the singlet biradical character in the ground state because of quinoid skeletons in the center of molecules. As shown in Figure 20, the contribution of the biradical form would lead to aromatization in the central six-membered ring. The X-ray determined structure of **36** (R = H) gave strong bond length alternation in the central 5-6-5 core, indicative of a small contribution of the biradical form. Actually, the ¹H NMR spectrum of **36** shows sharp signals in the aromatic region and the optically determined HOMO–LUMO gap is relatively large (1.98 eV). Aryl-substituted derivatives were also prepared and field-effect transistor (FET) characteristics were measured for a single crystal⁷⁷ or thin-films.⁷⁸ The field-effect hole and electron mobilities of the 6,12-bis(pentafluorophenyl) derivative were 7×10^{-4} and 3×10^{-3} cm² V⁻¹ s⁻¹ in the single crystal state, respectively.

Full characterization of indeno[2,1-*a*]fluorene was achieved after the isolation of the air-stable 11,12-dimesityl derivative **37** in 2011 (Figure 21).⁷⁹ The singlet biradical character of indeno[2,1-*a*]fluorene is estimated to be 33% on the basis of the broken-symmetry UHF calculation. X-ray crystallographic analysis of **37** revealed that there is significant bond length alternation in the central *o*-quinoid moiety. The optical and electrochemical HOMO–LUMO gaps were determined to be 1.70 and 2.10 eV, respectively. These relatively large HOMO–LUMO gaps are consistent with the nonmagnetic behavior observed in the variable temperature ¹H NMR spectra.

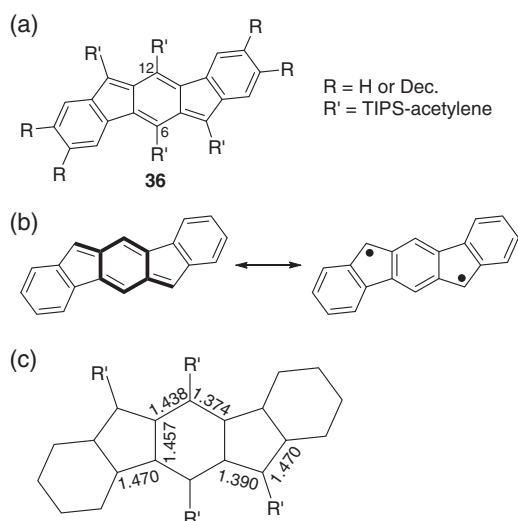


Figure 20. (a) TIPS-acetylene-substituted derivatives **36** of indeno[1,2-*b*]fluorene. (b) Resonance formula of indeno[1,2-*b*]fluorene. (c) X-ray determined bond lengths of **36** ($R = H$).

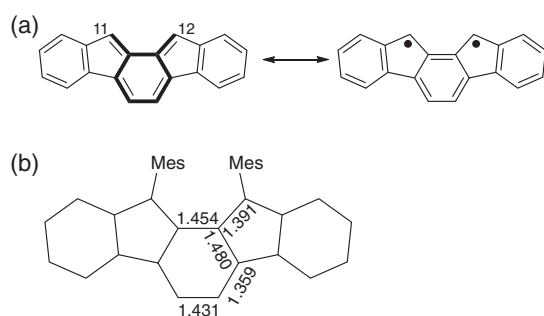


Figure 21. (a) Resonance formula of indeno[2,1-*a*]fluorene. (b) X-ray determined bond lengths of **37**.

Tobe et al. succeeded in full characterization of indeno[2,1-*b*]fluorene by the introduction of bulky mesityl groups at the most reactive carbons **38** (Figure 22).⁸⁰ Biradical character indeno[2,1-*b*]fluorene comes to 68% on the basis of the broken-symmetry UHF calculation, and this significant biradical character affects the appearance of ¹H NMR signals of **38**. At room temperature, **38** showed only broad signals, and upon cooling, progressive line sharpening was observed. The signal broadening is caused by a thermally accessible triplet species, which was detected by solid-state ESR spectra. The ΔE_{S-T} was determined to be 2120 K by SQUID measurements. It is noted that only the [2,1-*b*] isomer shows biradicaloid behavior. This is ascribable to that only one aromatic sextet can be drawn in the Kekulé form for the [2,1-*b*] isomer, whereas other isomers, except for the unknown [1,2-*a*] isomer, possess two sextets.

Haley et al. isolated three derivatives of indeno[2,1-*c*]fluorene **39a–39c** in 2013 (Figure 23).⁸¹ The X-ray determined structure shows strong bond length alternation in the central 5-6-5 core, indicative of small singlet biradical character. The electrochemical HOMO–LUMO gaps are relatively large (2.08 eV for **39a**, 1.73 eV for **39c**). Sharp ¹H and ¹³C NMR signals also support the small biradical character.

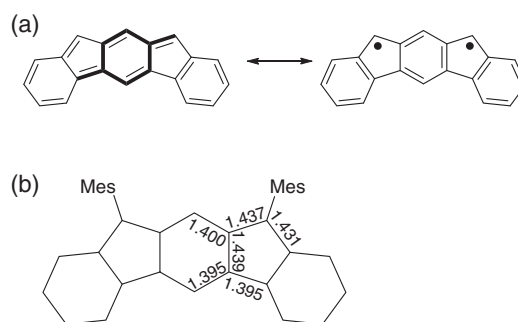


Figure 22. (a) Resonance formula of indeno[2,1-*b*]fluorene. (b) X-ray determined bond lengths of **38**.

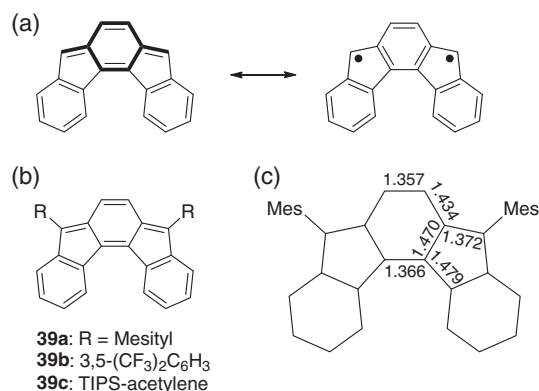


Figure 23. (a) Resonance formula of indeno[2,1-*c*]fluorene. (b) Three derivatives of indeno[2,1-*c*]fluorene. (c) X-ray determined bond lengths of **39a**.

Zethrenes. Interests in connection with the singlet biradical character were first invoked by Nakano et al. They pointed out potential singlet biradical character in zethrene and its larger homologues by theoretical calculations based on the spin-projected UHF theory.⁸² Due to the biradical character, a large static second-order hyperpolarizability (γ)⁸² and a high singlet fission efficiency⁸³ are expected for zethrene.

The parent zethrene (**40**) was first prepared by Clar in 1955 through a long step synthetic route.⁸⁴ The development of a more efficient synthesis and characterization by X-ray analysis were achieved by Wu and Tobe in 2010.⁸⁵ From the determined structure, the ground state of zethrene can be best represented by the structural formula described in Figure 24, indicating negligible singlet biradical character. Sharp NMR signals support the closed-shell character. Zethrene gives an intense absorption peak at 544 nm (ϵ 42900) in a benzene solution accompanied by fluorescence (Φ_{PL} 0.34) at 571 nm.

A larger homologue, which has seven six-membered rings, of zethrene is called heptazethrene. The large difference in chemical structure between zethrene and heptazethrene is that heptazethrene contains a *p*-quinoid skeleton. The parent heptazethrene (**41a**) was prepared by Clar in 1962,⁸⁶ but its high reactivity prohibited reliable characterization. Kinetically protected heptazethrene (**41b**) was isolated in 2012 by Wu et al.⁸⁷ **41b** showed an intense absorption band at 634 nm together with a weak fluorescence at 704 nm. The ¹H NMR spectrum gave

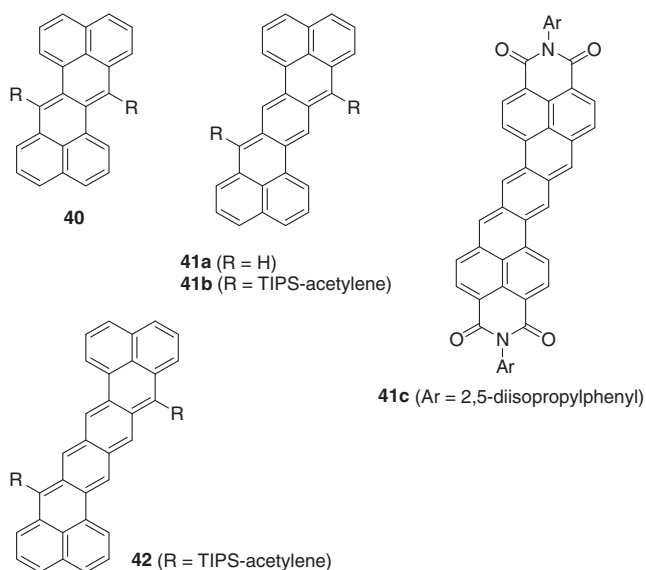


Figure 24. Zethrene family.

sharp signals from the main core rings, indicating the closed-shell character. The optically and electrochemically determined HOMO–LUMO gaps are relatively large (1.46 and 1.82 eV, respectively). Interestingly, the attachment of diimide groups at both end of heptazethrene led to biradicaloid behavior.⁸⁸ This derivative **41c** showed no ¹HNMR signals in the aromatic region at room temperature.

The longest molecule so far in the zethrene family is octazethrene, which was isolated in crystalline form by introducing TIPS acetylene groups at the reactive site.⁸⁷ This derivative **42** showed biradicaloid behavior; broad ¹HNMR signals in the aromatic region, small ΔE_{S-T} (16.2 kJ mol⁻¹), and an ESR signal in the solid state. The amount of singlet biradical character (γ) was estimated to be 43% by a broken symmetry UCAM-B3LYP calculation.

Experimental Determination of Singlet Biradical Character

As mentioned above, the NOON analysis based on CASSCF or broken symmetry UDFT/UHF calculations is a good index of singlet biradical character, whereas the NOON value depends on the methods and levels of calculation. Nakano et al. demonstrated that the amount of singlet biradical character (γ) can be estimated experimentally from the equation $\gamma = 1 - 4|t|/(U^2 + 16t^2)^{1/2}$, where U represents the difference between on-site and inter-site Coulomb integrals, and t is a transfer integral, using the localized natural orbital basis.⁸⁹ This formula is alternatively expressed as

$$\gamma = 1 - \sqrt{1 - \left(\frac{E_{S1u,S1g} - E_{T1u,S1g}}{E_{S2g,S1g}} \right)^2} \quad (1)$$

where $E_{S2g,S1g}$, $E_{S1u,S1g}$, and $E_{T1u,S1g}$ correspond to the excitation energies of the higher singlet state of the g symmetry (two-photon allowed excited state), of the lower singlet state with u symmetry (one-photon allowed excited state), and of the triplet state with u symmetry, respectively. These parameters can be determined experimentally from two-photon absorption (TPA),

UV–vis–NIR, and ESR (or phosphorescence, SQUID) measurements, respectively. Actually, the γ value experimentally estimated for a tetra-*tert*-butyl derivative of **7** was 34%, which is in good agreement with the value calculated by a broken-symmetry UB3LYP calculation ($\gamma = 37\%$).

Conclusion

It is suggested that singlet biradical molecules would show a high efficiency in the singlet fission process, which is expected to improve the photovoltaic characteristics.^{83,90–95} Furthermore, theoretical studies on nonlinear optics by Nakano et al. have revealed that singlet biradical molecules are promising candidates for large second hyperpolarizability (γ).^{96,97} Indeed, large TPA cross sections ($\sigma^{(2)}$) were observed for singlet biradical compounds.⁹⁸ The application to such a novel optical property would be one of next challenges of singlet biradical studies. At the same time, it is quite certain that many fundamental issues remain to be answered. For instance, how can we figure out the characteristic feature of a compound that possesses small singlet biradical character?, because such a species usually behaves like a normal closed-shell compound. Studies on unusual reactivity (as seen in **3**) and intermolecular covalent bonding character (as seen in **8**) might lead to distinguishing features. A strong collaboration of syntheses, measurements, and theoretical treatments is essential for the formidable challenges.

References

- 1 M. Szwarc, *Discuss. Faraday Soc.* **1947**, *2*, 46.
- 2 M. Szwarc, *Nature* **1947**, *160*, 403.
- 3 C. J. Brown, A. C. Farthing, *Nature* **1949**, *164*, 915.
- 4 C. A. Coulson, D. P. Craig, A. Maccoll, A. Pullman, *Discuss. Faraday Soc.* **1947**, *2*, 36.
- 5 D. J. Williams, J. M. Pearson, M. Levy, *J. Am. Chem. Soc.* **1970**, *92*, 1436.
- 6 J. M. Pearson, H. A. Six, D. J. Williams, M. Levy, *J. Am. Chem. Soc.* **1971**, *93*, 5034.
- 7 Y. Yamakita, Y. Furukawa, M. Tasumi, *Chem. Lett.* **1993**, 311.
- 8 Y. Yamakita, M. Tasumi, *J. Phys. Chem.* **1995**, *99*, 8524.
- 9 T. Koenig, R. Wielesek, W. Snell, T. Balle, *J. Am. Chem. Soc.* **1975**, *97*, 3225.
- 10 P. G. Mahaffy, J. D. Wieser, L. K. Montgomery, *J. Am. Chem. Soc.* **1977**, *99*, 4514.
- 11 M. Bobrowski, P. Skurski, S. Freza, *Chem. Phys.* **2011**, *382*, 20.
- 12 A. E. Tschitschibabin, *Ber. Dtsch. Chem. Ges.* **1907**, *40*, 1810.
- 13 E. Müller, I. Müller-Rodloff, *Justus Liebigs Ann. Chem.* **1935**, *517*, 134.
- 14 C. A. Hutchison, Jr., A. Kowalsky, R. C. Pastor, G. W. Wheland, *J. Chem. Phys.* **1952**, *20*, 1485.
- 15 H. S. Jarrett, G. J. Sloan, W. R. Vaughan, *J. Chem. Phys.* **1956**, *25*, 697.
- 16 D. C. Reitz, S. I. Weissman, *J. Chem. Phys.* **1960**, *33*, 700.
- 17 H. M. McConnell, *J. Chem. Phys.* **1960**, *33*, 1868.
- 18 R. K. Waring, Jr., G. J. Sloan, *J. Chem. Phys.* **1964**, *40*, 772.
- 19 H.-D. Brauer, H. Stieger, J. S. Hyde, L. D. Kispert, G. R. Luckhurst, *Mol. Phys.* **1969**, *17*, 457.
- 20 L. K. Montgomery, J. C. Huffman, E. A. Jurczak, M. P.

- Grendze, *J. Am. Chem. Soc.* **1986**, *108*, 6004.
- 21 M. P. Cava, R. H. Schlessinger, *J. Am. Chem. Soc.* **1963**, *85*, 835.
- 22 M. P. Cava, R. H. Schlessinger, *Tetrahedron* **1965**, *21*, 3073.
- 23 V. Boekelheide, G. K. Vick, *J. Am. Chem. Soc.* **1956**, *78*, 653.
- 24 J. Kolc, J. Michl, *J. Am. Chem. Soc.* **1970**, *92*, 4147.
- 25 J. Downing, V. Dvořák, J. Kolc, A. Manzara, J. Michl, *Chem. Phys. Lett.* **1972**, *17*, 70.
- 26 J. Kolc, J. Michl, *J. Am. Chem. Soc.* **1973**, *95*, 7391.
- 27 Recent reviews on biradicals: a) M. Abe, *Chem. Rev.* **2013**, *113*, 7011. b) Z. Sun, Z. Zeng, J. Wu, *Chem.—Asian J.* **2013**, *8*, 2894. c) Z. Sun, Z. Zeng, J. Wu, *Acc. Chem. Res.* **2014**, *47*, 2582.
- 28 D. Döhnert, J. Koutecký, *J. Am. Chem. Soc.* **1980**, *102*, 1789.
- 29 L. Noodleman, *J. Chem. Phys.* **1981**, *74*, 5737.
- 30 K. Yamaguchi, T. Kawakami, Y. Takano, Y. Kitagawa, Y. Yamashita, H. Fujita, *Int. J. Quantum Chem.* **2002**, *90*, 370.
- 31 L. Salem, C. Rowland, *Angew. Chem., Int. Ed. Engl.* **1972**, *11*, 92.
- 32 V. Bonačić-Koutecký, J. Koutecký, J. Michl, *Angew. Chem., Int. Ed. Engl.* **1987**, *26*, 170.
- 33 T. Kubo, A. Shimizu, M. Sakamoto, M. Uruichi, K. Yakushi, M. Nakano, D. Shiomi, K. Sato, T. Takui, Y. Morita, K. Nakasuji, *Angew. Chem., Int. Ed.* **2005**, *44*, 6564.
- 34 A. Shimizu, M. Uruichi, K. Yakushi, H. Matsuzaki, H. Okamoto, M. Nakano, Y. Hirao, K. Matsumoto, H. Kurata, T. Kubo, *Angew. Chem., Int. Ed.* **2009**, *48*, 5482.
- 35 A. Shimizu, T. Kubo, M. Uruichi, K. Yakushi, M. Nakano, D. Shiomi, K. Sato, T. Takui, Y. Hirao, K. Matsumoto, H. Kurata, Y. Morita, K. Nakasuji, *J. Am. Chem. Soc.* **2010**, *132*, 14421.
- 36 A. Shimizu, Y. Hirao, K. Matsumoto, H. Kurata, T. Kubo, M. Uruichi, K. Yakushi, *Chem. Commun.* **2012**, *48*, 5629.
- 37 R. Schmidt, H.-D. Brauer, *Angew. Chem., Int. Ed. Engl.* **1971**, *10*, 506.
- 38 Z. Zeng, Y. M. Sung, N. Bao, D. Tan, R. Lee, J. L. Zafra, B. S. Lee, M. Ishida, J. Ding, J. T. L. Navarrete, Y. Li, W. Zeng, D. Kim, K.-W. Huang, R. D. Webster, J. Casado, J. Wu, *J. Am. Chem. Soc.* **2012**, *134*, 14513.
- 39 R. West, J. A. Jorgenson, K. L. Stearley, J. C. Calabrese, *J. Chem. Soc., Chem. Commun.* **1991**, 1234.
- 40 A. Reibmann, J. Zhou, P. Schuler, H. B. Stegmann, A. Rieker, *J. Chem. Res., Synop.* **1996**, 318.
- 41 A. Reibmann, J. Zhou, P. Schuler, A. Rieker, H. B. Stegmann, *J. Chem. Soc., Perkin Trans. 2* **1997**, 1615.
- 42 K. Zhang, K.-W. Huang, J. Li, J. Luo, C. Chi, J. Wu, *Org. Lett.* **2009**, *11*, 4854.
- 43 A. Ueda, S. Nishida, K. Fukui, T. Ise, D. Shiomi, K. Sato, T. Takui, K. Nakasuji, Y. Morita, *Angew. Chem., Int. Ed.* **2010**, *49*, 1678.
- 44 T. Takahashi, K. Matsuo, K. Takimiya, T. Otsubo, Y. Aso, *J. Am. Chem. Soc.* **2005**, *127*, 8928.
- 45 R. P. Ortiz, J. Casado, V. Hernández, J. T. L. Navarrete, P. M. Viruela, E. Ortí, K. Takimiya, T. Otsubo, *Angew. Chem., Int. Ed.* **2007**, *46*, 9057.
- 46 E. Clar, *The Aromatic Sextet*, Wiley, London, **1972**.
- 47 M. Bendikov, H. M. Duong, K. Starkey, K. N. Houk, E. A. Carter, F. Wudl, *J. Am. Chem. Soc.* **2004**, *126*, 7416.
- 48 R. Mondal, B. K. Shah, D. C. Neckers, *J. Am. Chem. Soc.* **2006**, *128*, 9612.
- 49 M. M. Payne, S. R. Parkin, J. E. Anthony, *J. Am. Chem. Soc.* **2005**, *127*, 8028.
- 50 B. Purushothaman, M. Bruzek, S. R. Parkin, A.-F. Miller, J. E. Anthony, *Angew. Chem., Int. Ed.* **2011**, *50*, 7013.
- 51 A. Shimizu, Y. Hirao, T. Kubo, M. Nakano, E. Botek, B. Champagne, *AIP Conf. Proc.* **2012**, *1504*, 399.
- 52 L. B. Roberson, J. Kowalik, L. M. Tolbert, C. Kloc, R. Zeis, X. Chi, R. Fleming, C. Wilkins, *J. Am. Chem. Soc.* **2005**, *127*, 3069.
- 53 L. Zöphel, R. Berger, P. Gao, V. Enkelmann, M. Baumgarten, M. Wagner, K. Müllen, *Chem.—Eur. J.* **2013**, *19*, 17821.
- 54 Y. Hirao, A. Konishi, K. Matsumoto, H. Kurata, T. Kubo, *AIP Conf. Proc.* **2012**, *1504*, 863.
- 55 A. Konishi, Y. Hirao, M. Nakano, A. Shimizu, E. Botek, B. Champagne, D. Shiomi, K. Sato, T. Takui, K. Matsumoto, H. Kurata, T. Kubo, *J. Am. Chem. Soc.* **2010**, *132*, 11021.
- 56 J. Kruszewski, T. M. Krygowski, *Tetrahedron Lett.* **1972**, *13*, 3839.
- 57 T. M. Krygowski, *J. Chem. Inf. Model.* **1993**, *33*, 70.
- 58 C. Angeli, M. Pastore, R. Cimiraaglia, *Theor. Chem. Acc.* **2007**, *117*, 743.
- 59 S. Di Motta, F. Negri, D. Fazzi, C. Castiglioni, E. V. Canesi, *J. Phys. Chem. Lett.* **2010**, *1*, 3334.
- 60 J. E. Douglas, B. S. Rabinovitch, F. S. Looney, *J. Chem. Phys.* **1955**, *23*, 315.
- 61 M. N. Glukhovtsev, R. D. Bach, S. Laiter, *THEOCHEM* **1997**, *417*, 123.
- 62 S. W. Slayden, J. F. Liebman, *Chem. Rev.* **2001**, *101*, 1541.
- 63 A. Konishi, Y. Hirao, K. Matsumoto, H. Kurata, R. Kishi, Y. Shigetani, M. Nakano, K. Tokunaga, K. Kamada, T. Kubo, *J. Am. Chem. Soc.* **2013**, *135*, 1430.
- 64 M. Pan, E. C. Girão, X. Jia, S. Bhaviripudi, Q. Li, J. Kong, V. Meunier, M. S. Dresselhaus, *Nano Lett.* **2012**, *12*, 1928.
- 65 C. Tao, L. Jiao, O. V. Yazyev, Y.-C. Chen, J. Feng, X. Zhang, R. B. Capaz, J. M. Tour, A. Zettl, S. G. Louie, H. Dai, M. F. Crommie, *Nat. Phys.* **2011**, *7*, 616.
- 66 Z. Hou, X. Wang, T. Ikeda, S.-F. Huang, K. Terakura, M. Boero, M. Oshima, M. Kakimoto, S. Miyata, *J. Phys. Chem. C* **2011**, *115*, 5392.
- 67 K. Suenaga, M. Koshino, *Nature* **2010**, *468*, 1088.
- 68 V. L. J. Joly, M. Kiguchi, S.-J. Hao, K. Takai, T. Enoki, R. Sumii, K. Amemiya, H. Muramatsu, T. Hayashi, Y. A. Kim, M. Endo, J. Campos-Delgado, F. López-Urías, A. Botello-Méndez, H. Terrones, M. Terrones, M. S. Dresselhaus, *Phys. Rev. B* **2010**, *81*, 245428.
- 69 K. Sugawara, T. Sato, S. Souma, T. Takahashi, H. Suematsu, *Phys. Rev. B* **2006**, *73*, 045124.
- 70 Y. Kobayashi, K. Fukui, T. Enoki, K. Kusakabe, *Phys. Rev. B* **2006**, *73*, 125415.
- 71 Y. Niimi, T. Matsui, H. Kambara, K. Tagami, M. Tsukada, H. Fukuyama, *Appl. Surf. Sci.* **2005**, *241*, 43.
- 72 Y. Kobayashi, K. Fukui, T. Enoki, K. Kusakabe, Y. Kaburagi, *Phys. Rev. B* **2005**, *71*, 193406.
- 73 K. Nakada, M. Fujita, G. Dresselhaus, M. S. Dresselhaus, *Phys. Rev. B* **1996**, *54*, 17954.
- 74 M. Fujita, K. Wakabayashi, K. Nakada, K. Kusakabe, *J. Phys. Soc. Jpn.* **1996**, *65*, 1920.

- 75 K. Tanaka, S. Yamashita, H. Yamabe, T. Yamabe, *Synth. Met.* **1987**, *17*, 143.
- 76 D. T. Chase, B. D. Rose, S. P. McClintock, L. N. Zakharov, M. M. Haley, *Angew. Chem., Int. Ed.* **2011**, *50*, 1127.
- 77 D. T. Chase, A. G. Fix, S. J. Kang, B. D. Rose, C. D. Weber, Y. Zhong, L. N. Zakharov, M. C. Lonergan, C. Nuckolls, M. M. Haley, *J. Am. Chem. Soc.* **2012**, *134*, 10349.
- 78 J. Nishida, S. Tsukaguchi, Y. Yamashita, *Chem.—Eur. J.* **2012**, *18*, 8964.
- 79 A. Shimizu, Y. Tobe, *Angew. Chem., Int. Ed.* **2011**, *50*, 6906.
- 80 A. Shimizu, R. Kishi, M. Nakano, D. Shiomi, K. Sato, T. Takui, I. Hisaki, M. Miyata, Y. Tobe, *Angew. Chem., Int. Ed. Engl.* **2013**, *52*, 6076.
- 81 A. G. Fix, P. E. Deal, C. L. Vonnegut, B. D. Rose, L. N. Zakharov, M. M. Haley, *Org. Lett.* **2013**, *15*, 1362.
- 82 M. Nakano, R. Kishi, A. Takebe, M. Nate, H. Takahashi, T. Kubo, K. Kamada, K. Ohta, B. Champagne, E. Botek, *Comput. Lett.* **2007**, *3*, 333.
- 83 T. Minami, M. Nakano, *J. Phys. Chem. Lett.* **2012**, *3*, 145.
- 84 E. Clar, K. F. Lang, H. Schulz-Kiesow, *Chem. Ber.* **1955**, *88*, 1520.
- 85 T.-C. Wu, C.-H. Chen, D. Hibi, A. Shimizu, Y. Tobe, Y.-T. Wu, *Angew. Chem., Int. Ed.* **2010**, *49*, 7059.
- 86 E. Clar, I. A. Macpherson, *Tetrahedron* **1962**, *18*, 1411.
- 87 Y. Li, W.-K. Heng, B. S. Lee, N. Aratani, J. L. Zafra, N. Bao, R. Lee, Y. M. Sung, Z. Sun, K.-W. Huang, R. D. Webster, J. T. L. Navarrete, D. Kim, A. Osuka, J. Casado, J. Ding, J. Wu, *J. Am. Chem. Soc.* **2012**, *134*, 14913.
- 88 Z. Sun, K.-W. Huang, J. Wu, *J. Am. Chem. Soc.* **2011**, *133*, 11896.
- 89 K. Kamada, K. Ohta, A. Shimizu, T. Kubo, R. Kishi, H. Takahashi, E. Botek, B. Champagne, M. Nakano, *J. Phys. Chem. Lett.* **2010**, *1*, 937.
- 90 M. W. B. Wilson, A. Rao, J. Clark, R. S. S. Kumar, D. Brida, G. Cerullo, R. H. Friend, *J. Am. Chem. Soc.* **2011**, *133*, 11830.
- 91 P. M. Zimmerman, F. Bell, D. Casanova, M. Head-Gordon, *J. Am. Chem. Soc.* **2011**, *133*, 19944.
- 92 M. B. Smith, J. Michl, *Chem. Rev.* **2010**, *110*, 6891.
- 93 T. S. Kuhlman, J. Kongsted, K. V. Mikkelsen, K. B. Møller, T. I. Sølling, *J. Am. Chem. Soc.* **2010**, *132*, 3431.
- 94 P. M. Zimmerman, Z. Zhang, C. B. Musgrave, *Nat. Chem.* **2010**, *2*, 648.
- 95 I. Paci, J. C. Johnson, X. Chen, G. Rana, D. Popović, D. E. David, A. J. Nozik, M. A. Ratner, J. Michl, *J. Am. Chem. Soc.* **2006**, *128*, 16546.
- 96 M. Nakano, *Excitation Energies and Properties of Open-Shell Singlet Molecules: Applications to a New Class of Molecules for Nonlinear Optics and Singlet Fission*, Springer International Publishing, **2014**. doi:10.1007/978-3-319-08120-5.
- 97 M. Nakano, R. Kishi, T. Nitta, T. Kubo, K. Nakasuji, K. Kamada, K. Ohta, B. Champagne, E. Botek, K. Yamaguchi, *J. Phys. Chem. A* **2005**, *109*, 885.
- 98 K. Kamada, K. Ohta, T. Kubo, A. Shimizu, Y. Morita, K. Nakasuji, R. Kishi, S. Ohta, S. Furukawa, H. Takahashi, M. Nakano, *Angew. Chem., Int. Ed.* **2007**, *46*, 3544.